A simple algorithm to estimate evapotranspiration from DAIS data: Application to the DAISEX campaigns

J.A. Sobrino, M. Gomez, J.C. Jimenez-Munoz, Albert Olioso, A. Chehbouni

A simple algorithm to estimate evapotranspiration from DAIS data: Application to the DAISEX campaigns

J.A. Sobrino[a,*], M. Gómez[a], J.C. Jiménez-Muñoz[a], A. Olioso[b], G. Chehbouni[c]

[a]*Department of Thermodynamics, Faculty of Physics, University of Valencia, 50 Dr Moliner, 46100 Burjassot, Spain*
[b]*INRA Bioclimatologie, Domaine Saint-Paul, Avignon, France*
[c]*CESBIO (CNES-CNRS-IRD-UPS), Toulouse, France*

Abstract

The knowledge of evapotranspiration is of great interest in many applications such as assessing irrigation water use. In this paper, a methodology is presented to estimate evapotranspiration using the surface energy balance model S-SEBI (Simplified Surface Energy Balance Index) and the evaporative fraction. The method is applicable under the assumptions of constant atmospheric conditions and sufficient wet and dry pixels over the image. The model uses remotely sensed parameters such as albedo, MSAVI (Modified Soil Adjusted Vegetation Index) and surface temperature and emissivity images. The methodology has been applied over the Barrax test site located in the province of Albacete (Castilla La Mancha, Spain), in the framework of the DAISEX (Digital Airborne Imaging Spectrometer Experiment) campaigns carried out by ESA (European Space Agency). Net radiation, soil heat fluxes and evapotranspiration have been obtained from DAIS images for alfalfa, corn and grass plots. The results show that alfalfa plot gives the highest values, around 5 mm d^{-1}, whereas corn plot gives the lowest, around 3.5 mm d^{-1}. The proposed methodology leading to an accuracy for the daily evapotranspiration lower than 1 mm d^{-1}.

Keywords: Evapotranspiration; Evaporative fraction; Net radiation flux; Soil heat flux; DAIS; S-SEBI

1. Introduction

Evaporation is the process whereby liquid water is converted to water vapour and removed from the evaporating surface. Transpiration consists of the vaporisation of liquid water contained in plant tissues and the vapour removal to the atmosphere. The combination of the two separate processes whereby water is lost on the one hand from the soil surface by evaporation and on the other hand from the crop by transpiration is referred to as evapotranspiration (ET) (Allen et al., 1998). Knowledge of crop evapotranspiration is very important, because it allows optimisation of the irrigation water use in arid and semi-arid regions where water shortage is a problem. The estimation of evapotranspiration is of great importance for agricultural, hydrological and climatic studies, as it constitutes a major part of the hydrological cycle. Conventional

* Corresponding author. Fax: +34 96 3543099.
E-mail addresses: sobrino@uv.es (J.A. Sobrino), monica.gomez@uv.es (M. Gómez), juancar.jimenez@uv.es (J.C. Jiménez-Muñoz), olioso@avignon.inra.fr (A. Olioso), ghani@cesbio.cnes.fr (G. Chehbouni).

doi:10.1016/j.jhydrol.2005.03.027

ground-based methods for estimating evapotranspiration such as the Bowen ratio, provide accurate measurements over a homogeneous area surrounding the instrument, but the results are not applicable to large diverse areas. Significant improvements are expected from mapping of the spatial distribution of evapotranspiration using remote sensing.

In this paper, a simple algorithm to estimate the evapotranspiration from DAIS (Digital Airborne Imaging Spectrometer) images is presented. The images were obtained in the framework of DAISEX (Digital Airborne Imaging Spectrometer Experiments) campaigns, a series of experiments supported by ESA (European Space Agency) and achieved in 1998 (DAISEX-98), 1999 (DAISEX-99) and 2000 (DAISEX-00) in Barrax (39°3′N, 2°6′W), Castilla La Mancha (Spain). The description of the DAISEX campaigns and the DAIS sensor as well as the Barrax test site has been given below.

2. Methodology

On the basis of the S-SEBI (Simplified Surface Energy Balance Index) model developed by Roerink et al. (2000), the evapotranspiration (ET) can be estimated using the following equation

$$\mathrm{LET_i} = \Lambda(R_{\mathrm{ni}} - G_{\mathrm{i}}) \tag{1}$$

where $\mathrm{LET_i}$ is the instantaneous latent heat flux (W m^{-2}), Λ is the evaporative fraction, R_{ni} is the instantaneous net radiation flux (W m^{-2}) and G_{i} is the instantaneous soil heat flux (W m^{-2}). The methodology proposed in the paper is summarized in Fig. 1. Next, we give the expressions for the estimation of the different terms involved in Eq. (1).

2.1. Net radiation flux

The instantaneous net radiation flux can be obtained according to the following equation (Sobrino et al., 2000)

$$R_{\mathrm{ni}} = (1-\alpha)R_{\mathrm{c}\lambda\downarrow} + \varepsilon R_{\mathrm{g}\lambda\downarrow} - \varepsilon\sigma T_{\mathrm{S}}^4 \tag{2}$$

where α is the albedo, $R_{\mathrm{c}\lambda\downarrow}$ is the incoming shortwave radiation (W m^{-2}), $R_{\mathrm{g}\lambda\downarrow}$ is the incoming longwave radiation (W m^{-2}), σ is the Stefan Boltzman constant, ε the surface emissivity, and T_{S} the surface temperature (K). In order to estimate daily values,

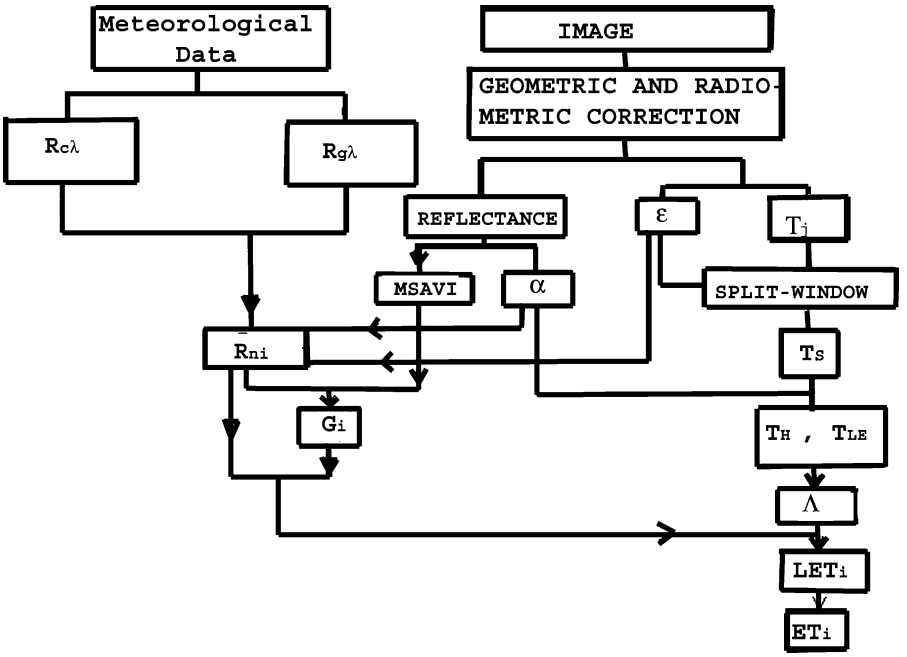

Fig. 1. Flowchart to obtain evapotranspiration.

the procedure proposed by Seguin and Itier (1983) has been used. According to these authors the ratio between daily and instantaneous net radiation is constant for a given time. For example, at midday (12:00 solar time) in summer the following expression can be used:

$$\frac{R_{nd}}{R_{ni}} = 0.30 \pm 0.03 \quad (3)$$

For instantaneous values not acquired at midday in summer, the ratio between R_{nd} and R_{ni} needs to be recalculated (Wassenaar et al., 2002).

2.1.1. Albedo

The ratio of the solar radiative flux that is reflected from a surface to the flux intercepted by the surface is called albedo. According to Saunders (1990), the surface albedo has been calculated using the visible and near infrared (NIR) channels according to the following equation

$$\alpha = \frac{1}{2}(\rho_{RED} + \rho_{NIR}) \quad (4)$$

where ρ_{RED} and ρ_{NIR} are, respectively, the RED and NIR reflectances calculated in our case using DAIS channels 10 (0.66 μm) and 22 (0.87 μm), respectively.

2.1.2. Surface temperature and emissivity

In order to apply Eq. (2), land surface temperature (T_S) and emissivity are needed. In this paper, the split-window algorithm proposed by Sobrino et al. (2004) and adapted to DAIS channels has been used

$$T_S = T_{77} + 2.937(T_{77} - T_{78}) + 0.8193(T_{77} - T_{78})^2 - 0.3284 + (72.094 - 13.864W) \times (1 - \varepsilon) + (-119.592 + 25.136W)\Delta\varepsilon \quad (5)$$

where T_{77} and T_{78} are the at-sensor or brightness temperatures (in K) for DAIS thermal channels 77 and 78, $\varepsilon = (\varepsilon_{77} + \varepsilon_{78})/2$ and $\Delta\varepsilon = (\varepsilon_{77} - \varepsilon_{78})$ are the mean surface effective emissivity and the spectral emissivity difference, respectively, and W is the total atmospheric water vapour content (in g cm^{-2}).

Land surface emissivity has been estimated from DAIS data using the NEM (Normalized Emissivity Method), developed by Gillespie (1985), following the procedure explained in Sobrino et al. (2004). Despite the NEM is capable of providing T_S, in this paper, we have obtained T_S from Eq. (5) which give better results specially for wet atmospheres (Sobrino and Jiménez-Muñoz, 2003). The accuracy of T_S and emissivity obtained from Eq. (5) and the NEM method is better than 1.5 K and 0.01, respectively.

2.2. Soil heat flux

The soil heat flux can be estimated from the net radiation and the MSAVI (Modified Soil Adjusted Vegetation Index) values according to

$$G_i = R_{ni} 0.5 \exp(-2.13\ \mathrm{MSAVI}) \quad (6)$$

where MSAVI is given by (Qi et al., 1994):

$$\mathrm{MSAVI} = \frac{2\rho_{NIR} + 1 - \sqrt{(2\rho_{NIR} + 1)^2 - 8(\rho_{NIR} - \rho_{RED})}}{2} \quad (7)$$

As was explained before, ρ_{RED} and ρ_{NIR} are, respectively, the RED and NIR reflectances calculated using DAIS channels 10 (0.66 μm) and 22 (0.87 μm).

2.3. Evaporative fraction

According to Roerink et al. (2000), the evaporative fraction (Λ) is given by

$$\Lambda = \frac{T_H - T_S}{T_H - T_{LET}} \quad (8)$$

where T_S is the land surface temperature and T_H and T_{LET} are two temperatures obtained according to the scheme given in Fig. 2. It should be noticed that Eq. (8) is only applicable when the atmospheric conditions are constant over the images and sufficient wet and dry pixels are present. From the analysis of the Fig. 2 it is observed an approximately constant surface temperature (T_S) for low albedo values. This concern water saturated surfaces like open water and irrigated lands, where all available energy is used in evaporation process. On the other hand, for higher albedo values the figure shows an increase of T_S with albedo. Thus, from A to B the temperature increases with albedo because of the change in the surface temperature is a result of the decrease of

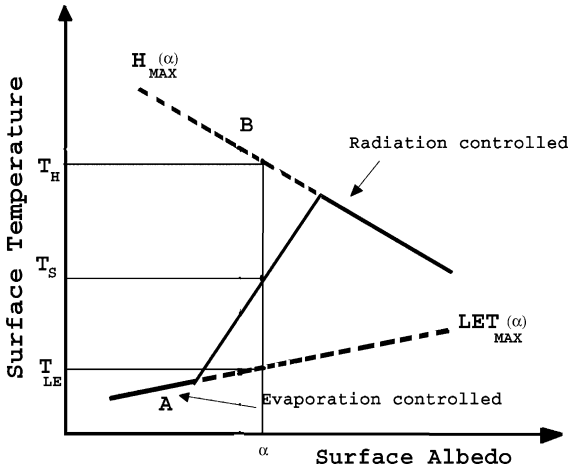

Fig. 2. Surface temperature versus surface albedo. H is the sensible heat flux, LET is the latent heat flux and α is the albedo (adapted from Roerink et al., 2000).

the evaporation as a consequence of less soil moisture availability. Here, the surface temperature increase in excess due to sensible heat flux exceeds the decrease in net radiation due to the increase of albedo. Here, the surface temperature is said 'controlled evaporation'. Finally, the surface temperature (from B) decreases with increasing albedo. This is due to the fact that soil moisture has decreased to such an extent that no evaporation can take place in this case, and all available energy is used to heat the surface. Thus to the increase of albedo, the available energy decreases as a result of the decrease in net radiation. Here, the surface temperature is said 'controlled radiation' (Roerink et al., 2000). In this way, T_{LET} is obtained when $H_{\mathrm{i}}=0$, and therefore, $\mathrm{LET}_{\mathrm{max\ i}}(\alpha)=R_{\mathrm{ni}}-G_{\mathrm{i}}$; and T_{H} when $\mathrm{LET}_{\mathrm{i}}=0$, and for this case, $H_{\mathrm{max\ i}}(\alpha)=R_{\mathrm{ni}}-G_{\mathrm{i}}$.

2.4. Evapotranspiration

Evapotranspiration can be easily obtained from Eq. (1) once the net radiation, the soil heat flux and the evaporative fraction are known. Estimation of evapotranspiration daily values $\mathrm{ET_d}$ (in mm d^{-1}) requires the integration of the latent heat flux over the whole day, with L the latent heat of vaporization (2.45 MJ kg^{-1}). When LET values are instantaneous, as is the case of remote sensing images, then daily values can be obtained by assuming that the evaporative fraction at the daily scale is similar to the instantaneous value derived from Eq. (8) at the time of remote sensing data acquisition (Bastiaansen, 2000). In this way, writing Eq. (1) for daily and instantaneous values the following equation is obtained

$$\frac{\mathrm{LET_d}}{\mathrm{LET_i}}=\frac{\Lambda_{\mathrm{d}}}{\Lambda_{\mathrm{i}}}\frac{(R_{\mathrm{nd}}-G_{\mathrm{d}})}{(R_{\mathrm{ni}}-G_{\mathrm{i}})}\approx\frac{(R_{\mathrm{nd}}-G_{\mathrm{d}})}{(R_{\mathrm{ni}}-G_{\mathrm{i}})} \tag{9}$$

and therefore, it is possible to express daily values as a function of instantaneous values according to

$$\mathrm{ET_d}=\mathrm{LET_i}\frac{R_{\mathrm{nd}}}{L(R_{\mathrm{ni}}-G_{\mathrm{i}})} \tag{10}$$

where the ground heat flux has been assumed close to zero at daily scale ($G_{\mathrm{d}}\approx 0$) and daily net radiation can be expressed in terms of instantaneous net radiation according to Eq. (3).

3. The DAISEX field campaigns

The main scientific objective of the DAISEX campaigns was to demonstrate the feasibility of quantitatively retrieving geo/biophysical variables by accounting for atmospheric effects while at the same time analysing the data for possible additional information on directional anisotropy. Bio/geophysical variables included the leaf area index (LAI), biomass, leaf water content, canopy height, chlorophyll content, surface temperatures and emissivity.

Since, accurate calibration and atmospheric corrections are essential to quantitatively retrieve these variables, in situ atmospheric measurements (needed to derive the atmospheric corrections) were performed in addition to field measurements for validating calibration and retrieval. Three airborne campaigns were organised over test sites in Spain, France and Germany in 1998, 1999 and 2000 exploiting a range of different airborne instruments (Müller and Hausold, 2001).

3.1. The DAIS sensor

The Digital Airborne Imaging Spectrometer, DAIS 7915 (or simply DAIS), is a 79 channel high resolution optical spectrometer which collects information from the Earth's surface in the 0.4–13 μm wavelengths region while scanning from an aircraft, electronically processes this data into digital format consisting of 16 bit words, and records these digital data on a cartridge recorder. The DAIS scan mechanism is a Kennedy type where a cubic polygon mirror scans the terrain below through the opened window hatch in the bottom of the aircraft. The scan mirror rotates anti-clockwise with respect to the aircraft heading to provide a ground element cross track scanning motion while the forward motion of the aircraft provides a requested line-by-line scan. The most relevant geometric parameters are the IFOV (Instantaneous Field of View), 3.3 mrad, and the swath angle, $\pm 26°$. From the 79 channels, six works in the 8–13 μm region (from 74 to 79, with the next effective wavelengths: 8.747, 9.648, 10.482, 11.266, 11.997 and 12.668 μm, respectively) with a bandwidth of 0.9 μm. They can be used for the retrieval of temperature and emissivity of land surface objects (Müller and Hausold, 2001). The principal characteristics of the DAIS sensor are shown in Table 1.

Table 1
Principal characteristics for DAIS-7915 sensor

Spectrometer characteristics			
Wavelength range (nm)	No. bands	Bandwidth	Detector
450–1050	32	25 nm	Si
1500–1800	8	45 nm	InSb
1900–2450	32	25 nm	InSb
3000–5000	1	2.0 μm	MCT
8700–12300	6	0.9 μm	MCT
Geometric parameters			
IFOV: 3.3 mrad Swath angle: $\pm 26°$ Image pixels per line: 512 Spatial Resolution: 2–20 m (depending on the flight altitude)			
Radiometric parameters			
Sensibility	VIS/NIR: NER <0.25 W m^{-2} sr μm SWIR: NER <0.25 W m^{-2} sr μm MIR/TIR: NET <0.1 K		
Dynamic range: 15 bit (no gain settings)			

3.2. The Barrax test site

The Barrax test site is situated in the west of the province of Albacete, 28 km from the capital town (39°3′N, 2°6′W; 700 m above sea level). The landscape in this area is flat with no change of elevation higher than 2 m over the whole area. Under Barrax area several aquiferous geological formations exit. These formations seem to be connected and form a regional groundwater body. The regional water table is about 20–30 m below the land surface. Nevertheless, there is some evidence that, at least locally, several perched aquifers exist with their water table between 4 and 7 m deep (Moreno et al., 2001).

The climate is of Mediterranean type, with heaviest rainfalls in spring and autumn and lowest in summer. It presents a high level of continentally, with quite sudden changes from cold months to warm months and high thermal oscillations in all seasons between the maximum and minimum daily temperatures. The rainfall statistics show that the mean annual rainfall is little more than 400 mm in most of the area, making La Mancha one of the driest regions in Europe. Precipitation is seasonal, with minimum in summer and high year-to-year variability. The dominant cultivation in the 10,000 ha area is approximately 65% dry land (of which 67% are winter cereals and 33% fallow land) and 35% irrigated land (corn 75%; barley/sunflower 15%, alfalfa 5%; onions 2.9%; vegetables 2.1%). The University of Castilla-La Mancha, owns the agroclimatologic station of Las Tiesas-Lisímetro (39°03′30″N; 2°05′24″W) in the study area of Barrax.

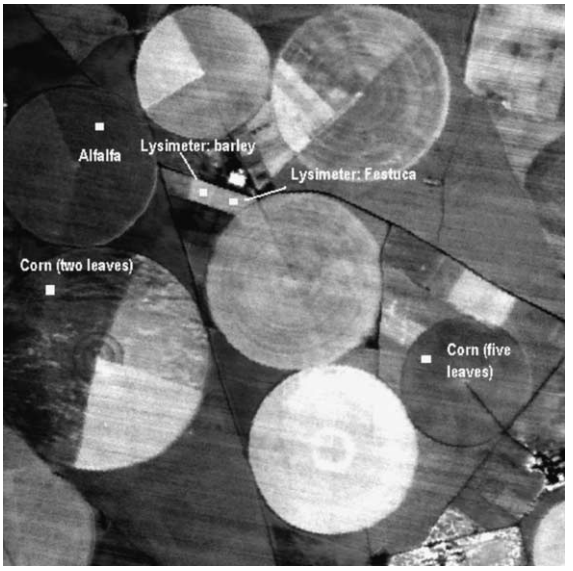

Fig. 3. DAIS image for the Barrax site with the different plots selected to estimate evapotranspiration.

Table 2
Meteorological data employed to determine the net radiation flux (where $R_{c\lambda\downarrow}$; and $R_{g\lambda\downarrow}$; are the incoming shortwave and longwave radiation, respectively)

Date	Time flight (GMT)	$R_{c\lambda\downarrow}$ (W m^{-2})	$R_{g\lambda\downarrow}$ (W m^{-2})
June 3	12:00	1010	354
	12:10	1008	355
June 4	8:00	548	318
	8:10	579	320
	15:00	797	357
	15:10	773	357

4. Results

In order to analyse the results obtained by applying the methodology proposed, five regions of 5×5 pixels (25 m^2) with different crops have been extracted from the DAIS images acquired over the Barrax test site: alfalfa, corn with five leaves, corn with two leaves, Festuca and barley (see Fig. 3). Table 2 shows the date and the time flight for the DAIS images used in this study, as well as the incoming shortwave and longwave radiation obtained from meteorological data and needed in order to estimate the net radiation from Eq. (2). Table 3 shows the T_H and T_{LET} values obtained for the different DAIS images as a function of surface albedo (see Section 2.3). Table 4 shows the results obtained for the different fluxes and the daily evapotranspiration by using the expressions explained in Section 2 and the data shown in Tables 2 and 3. And finally, Table 5 shows the instantaneous net radiation and soil heat fluxes measured in the Anchor Station, and the values estimated with the proposed method. The methodology has been tested using measured data from the lysimeter station located near the festuca and barley plots. The comparison between ET values obtained with the methodology proposed in the paper and the lysimeters measured values for 3 June 1999 on festuca (5.01 mm d^{-1}) and barley (5.35 mm d^{-1}) and for 4 June on festuca (4.59 mm d^{-1}) and barley (5.60 mm d^{-1}) shows a root mean square deviation (RMSD) of 1 mm d^{-1}. Daily net radiation, daily latent heat and instantaneous heat soil and fluxes have been also compared with meteorological data, showing a RMSD of 7, 26 and 40%, respectively. These RMSD values agree with the errors obtained from the sensitivity analysis (in which typical errors of 0.03 for

Table 3
Values of T_H, and T_{LET} for the different flights as a function of albedo (α)

Date	Time flight (GMT)	T_H (K)	T_{LET} (K)
03/06/99	12:00	$-37.5\alpha+350.0$	$17.5\alpha+290.0$
	12:10	$-55.0\alpha+360.0$	$12.5\alpha+290.0$
04/06/99	8:00	$-32.5\alpha+330.0$	$10.0\alpha+287.0$
	8:10	$-40.0\alpha+340.0$	$7.5\alpha+289.0$
	15:00	$-32.5\alpha+340.0$	$17.5\alpha+290.0$
	15:10	$-35.0\alpha+345.0$	$17.5\alpha+290.0$

T_{LET} is obtained when $H_i=0$, and therefore, $LET_{max\ i}(\alpha)=R_{ni}-G_i$; and T_H when $LET_i=0$, and for this case $H_{max\ i}(\alpha)=R_{ni}-G_i$ (see Section 2.3).

Table 4
Values of daily net radiation flux, R_{nd}/R_{ni}, instantaneous soil heat flux, evaporative fraction and daily evapotranspiration obtained from the proposed method and for the different plots extracted from DAIS images

Plot	Date/time flight (GMT)	R_{nd}/R_{ni}	R_{nd} (W m^{-2})	G_i (W m^{-2})	Λ	ET_d^{METHOD} (mm d^{-1})
Barley	June 3/12:00	0.27	174.12	47.67	0.72	4.09
	June 3/12:10	0.27	157.88	43.89	0.70	3.60
	June 4/8:00	0.52	178.22	30.48	0.87	4.98
	June 4/8:10	0.49	175.62	32.14	0.89	5.02
	June 4/15:00	0.36	186.86	29.42	0.72	4.47
	June 4/15:10	0.38	185.45	29.16	0.73	4.49
Festuca	June 3/12:00	0.27	174.73	46.67	0.62	3.54
	June 3/12:10	0.27	169.81	44.48	0.71	3.95
	June 4/8:00	0.52	169.39	34.15	0.73	3.90
	June 4/8:10	0.49	166.64	35.82	0.76	4.00
	June 4/15:00	0.36	189.23	33.56	0.67	4.18
	June 4/15:10	0.38	186.80	32.16	0.67	4.12
Alfalfa	June 3/12:00	0.27	159.10	15.37	0.88	4.81
	June 3/12:10	0.27	152.36	14.56	0.91	4.76
	June 4/8:00	0.52	147.26	10.83	0.96	4.79
	June 4/8:10	0.49	150.81	11.41	0.96	4.91
	June 4/15:00	0.36	173.41	10.86	0.91	5.44
	June 4/15:10	0.38	173.67	10.63	0.92	5.50
Corn (two leaves)	June 3/12:00	0.27	159.09	61.37	0.76	3.82
	June 3/12:10	0.27	150.49	58.59	0.76	3.61
	June 4/8:00	0.52	154.56	50.94	0.78	3.52
	June 4/8:10	0.49	143.19	48.10	0.80	3.37
	June 4/15:00	0.36	131.92	31.47	0.51	2.17
	June 4/15:10	0.38	144.65	36.11	0.60	2.77
Corn (five leaves)	June 3/12:00	0.27	161.39	63.11	0.70	3.56
	June 3/12:10	0.27	159.66	63.00	0.76	3.82
	June 4/8:00	0.52	143.61	47.69	0.74	3.10
	June 4/8:10	0.49	149.84	47.67	0.78	3.43
	June 4/15:00	0.36	159.43	43.89	0.56	2.85
	June 4/15:10	0.38	152.44	30.48	0.58	2.81

albedo, 1.5 K for temperature, 0.01 for emissivity and 5% for the incoming shortwave and longwave radiation have been considered).

Once the algorithm have been evaluated, it has been applied to DAIS images. Figs. 4 and 5 show, respectively, the daily evapotranspiration obtained from 4 June at 8:00 GMT on the Barrax site and the difference between daily evapotranspiration estimated for two consecutive flights. Fig. 4 shows the highest values for alfalfa and lowest values for corn plots and allows to distinguish the irrigated areas on the different plots. Fig. 5 shows little differences between the two consecutive flights, which gives some confidence on the developed methodology to obtain the evapotranspiration.

Table 5
Experimental and model values of R_{ni} and G_i for the Barrax test site

Date/time flight (GMT)	Method		Anchor station measure	
	R_{ni} (W m^{-2})	G_i (W m^{-2})	R_{ni} (W m^{-2})	G_i (W m^{-2})
June 3/12:00	464.0	53.5	570.0	54.0
June 3/12:10	498.4	54.6	567.0	54.0
June 4/8:00	315.7	67.2	277.0	13.0
June 4/8:10	296.0	50.3	297.0	16.0
June 4/15:00	333.6	32.4	400.0	48.0
June 4/15:10	364.0	40.9	384.0	46.0

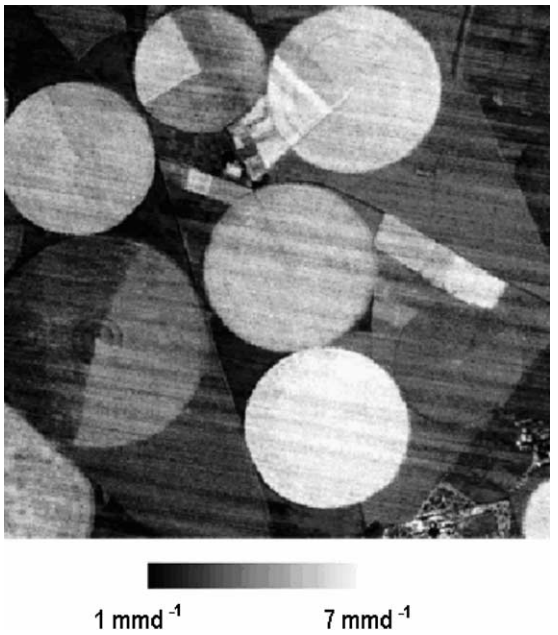

Fig. 4. Daily evapotranspiration (ET_d) image obtained from DAIS image on June 4th at 8:00 GMT.

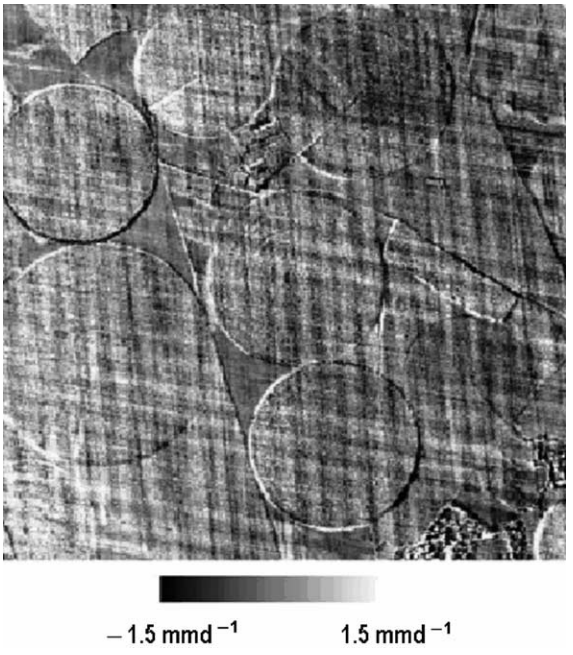

Fig. 5. Difference between daily evapotranspiration (ET_d) obtained from DAIS images on June 4th at 8:00 and 8:10 GMT.

5. Conclusions

In this paper, a simplified methodology in order to obtain daily evapotranspiration. The methodology has been applied to an experimental test site in Albacete (Spain) in which five plots have been selected (alfalfa, corn with two and five leaves, festuca and barley). The results show daily evapotranspiration can be obtained with an error lower than 1 mm d^{-1}. The main disadvantage of the methodology proposed is the requirement of extreme surface values over the image. Other methods as SEBAL shows better results in the daily evapotranspiration determination, but this method includes the determination of the roughness length, which is a difficult task. Further, studies are necessary in order to confirm the results presented in this paper.

Acknowledgements

We wish to thank the ESA (European Space Agency) for financial support (projects ESA-ESTEC 13053/NL/GD and 13390/NL/GD) and the DLR (German Optoelectronic Institute) for providing the DAIS images. We would also like to thank the European Union (EAGLE, Project SST3-CT-2003-502057) and the Ministerio de Ciencia y Tecnología (project REN2001-3105/CLI) for the financial support.

References

Allen, R.G., Pereira, L.S., Raes, D., Smith, M., 1998. Crop evapotranspiration—Guidelines for computing crop water requirements. FAO Irrigation and drainage paper 56, Rome.

Bastiaanssen, W.G.M., 2000. SEBAL-based sensible and latent heat fluxes in the irrigated Gediz Basin, Turkey. J. Hydrol. 229, 87–100.

Gillespie, A.R., 1985. Lhitologic mapping of silicate rocks using TIMS. The TIMS Data Users Workshop. JPL Publications pp. 86–38, see also 29–44.

Moreno, J., Calera, A., Caselles, V., Cisneros, J.M., Martinez-Lozano, J.A., Melia, J., Montero, F., Sobrino, J.A., 2001. The measurement programme at Barrax. DAISEX Final Results Workshop, ESTEC, Holland, 15–16 March 2001, ESA SP-499, pp. 43–51.

Müller, A., Hausold, A., 2001. The airborne imaging spectrometer data acquisition programme in 1998, 1999 and 2000. DAISEX Final Results Workshop, ESTEC, Holland, 15–16 March 2001, ESA SP-499, pp. 7–11.

Qi, J., Chehbouni, A., Huete, A.R., Kerr, Y.H., Sorooshian, S., 1994. A modified soil adjusted vegetation index (MSAVI). Remote Sensing Environ. 48, 119–126.

Roerink, G.J., Su, Z., Menenti, M., 2000. S-SEBI: a simple remote sensing algorithm to estimate the surface energy balance. Phys. Chem. Earth (B) 25 (2), 147–157.

Saunders, R.W., 1990. The determination of broad land surface albedo from AVHRR visible and near infrared radiances. Int. J. Remote Sensing 11, 49–67.

Seguin, B., Itier, B., 1983. Using midday surface temperature to estimate daily evaporation from satellite thermal IR data. Int. J. Remote Sensing 4 (2), 371–383.

Sobrino, J.A., Jiménez-Muñoz, J.C., 2003. Land surface temperature retrieval in the framework of the SPECTRA mission, Proceedings of Second SPECTRA Workshop, 28–30 October, STEC (Noordwijk, The Netherlands). ESA Publications.

Sobrino, J.A., Raissouni, N., Kerr, Y., Olioso, A., López-García, M.J., Belaid, A., El Kharraz, J., Cuenca, J., Dempere, L., 2000. In: Sobrino, J.A. (Ed.), Teledetección. Servicio de publicaciones, Universidad de Valencia, Valencia, Spain. ISBN: 84-37034220-8.

Sobrino, J.A., Jiménez-Muñoz, J.C., El Kharraz, J., Gomez, M., Romaguera, M., Soria, G., 2004. Single-channel and two-channel methods for land surface temperature retrieval from DAIS data and its application to the Barrax site. Int. J. Remote Sensing 25 (1), 215–230.

Wassennar, T., Olioso, A., Hasager, C., Jacob, F., Chehbouni, A., 2002. Estimation of evapotranspiration on heterogeneous pixels. In: Sobrino, J.A. (Ed.), First International Symposium on Recent Advances in Quantitative Remote Sensing, 16–20 September 2002. Publicacions de la Universitat de València, España, Valencia, Spain, pp. 458–465.